Ali Raza, University College London

Computational Characterisation of Amyloid-β 40 and 42 in Alzheimer's Disease

Overview. I spent 6 weeks in the Extreme Dynamics and Therapeutics Laboratory led by Dr Gabriella Heller, where I performed multi-scale simulations of Amyloid-β (Aβ), which aggregates within the brain tissue of patients with Alzheimer's disease and is considered a defining hallmark of the illness. Aβ exists in two forms: a toxic, aggregation-prone 42-residue variant (Aβ42, Figure 1) found in brain tissue of patients with Alzheimer's and a C-terminally truncated 40 residue variant, which aggregates more slowly (Aβ40, Figure 1). The aim of my research was to determine whether differences in the monomeric forms of the two peptides contribute to their varying aggregation rates, as changes in aggregation can be detected from the earliest stages of the self-association process, beginning with the pure monomeric species (1). This would allow a better understanding of which residues play a crucial role in Aβ aggregation and subsequently drive rational drug design efforts to block this process.

Figure 1. *A. Sequence of Aβ42 and AB40 with histidine residues highlighted.*

All atom molecular dynamics simulations (MD). I employed all atom metadynamics simulations using GROMACS (version 2022.5) patched with the PLUMED library (version 2.9.0) and the CHARMM22* (2) force field and TIP3P water model as these agree well with experimental data for Aβ42 (3). To enhance sampling, parallel bias metadynamics was used which involves deposition of artificial gaussian biases along a set of defined collective variables (CVs), encouraging the system to sample previously unexplored confirmations more quickly. Six identical CVs were used for both peptides, namely the α-helical content, the β-sheet content, the radius of gyration, the correlation between dihedral angles, the amount of hydrophobic contacts, and the amount of salt bridges (3). After collapsed structures of Aβ40 and Aβ42 were obtained using energy minimization simulations of linear peptides created using PyMol, the structures were simulated at 600 K using the NVT ensemble and 100 conformationally diverse replicas of each variant were extracted for production MD. The replicas were solvated with >10,000 water molecules, NaCl (0.137 M) and KCl ions (0.0027 M) were added, and a temperature of 278 K was used for subsequent simulations (to match experimental conditions). Charges in ionizable residues were set using a pH of 8. The replicas were energy minimized and equilibrated in the NVT and NPT ensembles for 1,000 nanoseconds each. Subsequently, production MD was started in the NPT ensemble using a timestep of 4 femtoseconds based on Hydrogen Mass Repartitioning (4). To date, around 15 μs worth of data has been collected for each AB40 and Aβ42, but not all CVs have reached convergence. Based on previous simulations of similar size, I expect to need around 30 μs. During the academic year, I plan to continue these simulations and monitor their convergence before final analysis.

Coarse grained MD. It has been previously reported that ionizable residues play a significant role in the conformations, binding, and phase behaviour of IDPs (5). I was curious to see if this could explain differences in aggregation propensities of AB40 and Aβ42 monomers. Only histidine residues, (with a pKa of ~6.3), can undergo a significant change in charge state populations in a physiologically relevant pH range of 6 to 8.5. Aβ has three histidine residues (positions 6, 13, and 14) that could potentially lead to a change in conformational properties of the peptide. These residues can take on a charge of either 0 or +1, leading to 8 different charge states and hence16 simulations in total for both peptides (Figure 2). Simulating all systems with all-atom MD was prohibitively computationally expensive for my summer project. Thus, to test this hypothesis, I turned to CALVADOS2, a coarse-grained MD model optimized to predict the confirmational properties and phase behaviour of IDPs at different charge states, salt concentrations, and temperatures (6, 7). I explored the ability of CALVADOS distinguish between the confirmational ensembles of different histidine charge states for Aβ40 and Aβ42. CALVADOS2 is a C_α-based model that treats each residue in a protein sequence as a single bead with a given mass and charge. Additionally, a stickiness parameter termed 'lambda' is assigned to each residue which is utilized in a Leonard-Jones like potential to model hydrophobic interactions between resides. Salt-screened electrostatic interactions are modelled using the Debye-Huckle potential and the solvent is treated implicitly.

AB40/AB42	H6	H13	H14
	0	0	0
	0	0	1
	0	1	0
	0	1	1
	1	0	0
	1	0	1
	1	1	0
	1	1	1

Figure 2. *Charge states of Aβ40 and Aβ42 based on permutations of histidine charges.*

CALVADOS2 simulations of all permutations of histidine charge states of Aβ40 and Aβ42 were carried out at 278K with an ionic strength of 0.1397 M for 1,000 ns using a timestep of 10 fs (8). After convergence was reached, conformational properties of the peptides for each simulation were analysed (Figure 3). All coarse-grained simulations predict the radius of gyration (R_g) for Aβ40 and Aβ42 to be ~1.7 nm with Aβ42 having a slightly larger R_g (Figure 3A). I plan to compare this with my all-atom simulations once convergence is reached. Distributions of end-to-end distance (Figure 3B), number of salt bridges (Figure 3C) and number of hydrophobic contacts (Figure 3D) in the monomeric peptides were also calculated but no differences between charge states were observed, as indicated by almost identical distributions and mean values. The only difference observed was Aβ42 having a higher number of hydrophobic contacts on account of having two extra C-terminal hydrophobic residues (Figure 3D, 3E). Similarly, there were no differences observed between charge states in the number of histidine-hydrophobic contacts and histidine-salt bridges (Figures 3F and 3G) using the CALVADOS model. We also assessed solvent accessibility of residues within the peptides but no significant differences between charge states were observed.

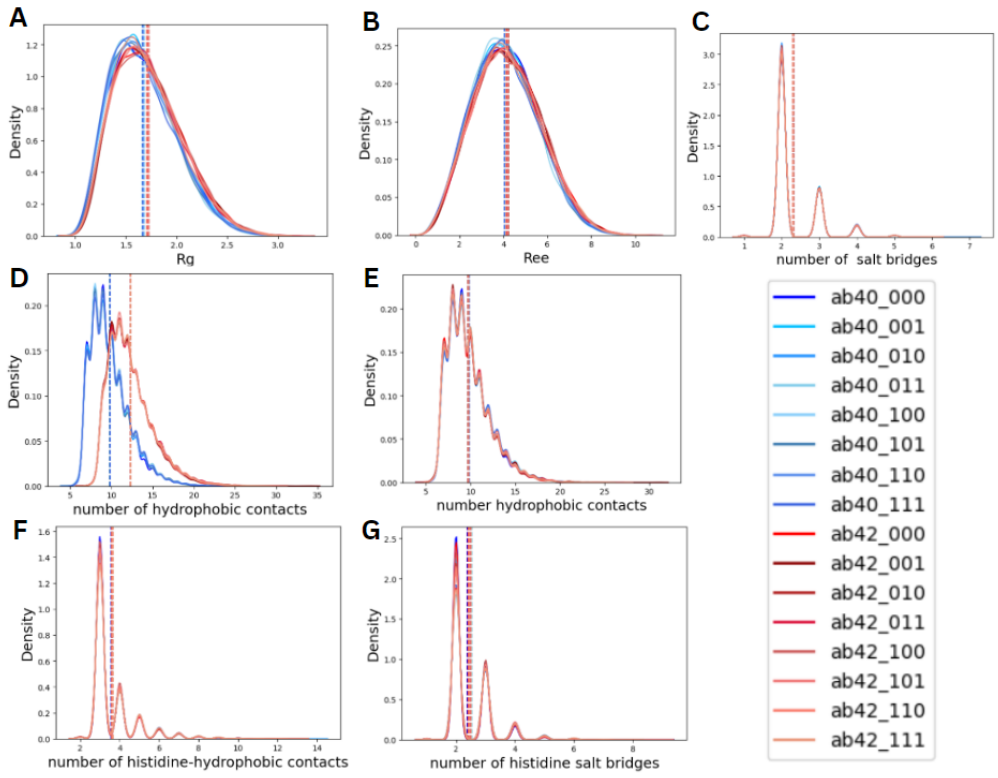

Figure 3. *Summary of results for CALVADOS2 simulations of all histidine charge states of Aβ40 and Aβ42 monomers. Kernal density estimation distributions of radius of gyration (R_g, A), end-to-end distance (R_{ee}, B), number of salt bridges (C), number of hydrophobic contacts for all residues in Aβ40 and Aβ42 (D), number of hydrophobic contacts considering all residues of Aβ40*

and only the first 40 residues of Aβ42 (E), number of histidine-salt bridges (F), and number of histidine-hydrophobic contacts (G). The dashed lines represent the means of the distributions.

Next steps. While my internship is over, I am continuing the MD simulations and hope to obtain converged trajectories results soon. Insights gained from these simulations would provide valuable information regarding Aβ42 aggregation mechanism which may direct rational drug design approaches to target monomeric Aβ42 and prevent its aggregation. The internship allowed me to learn about performing all-atom and coarse-grained MD simulations, enhanced sampling techniques, the physics behind these simulations, analysis of convergence using blocking, and general analysis of simulation trajectories using different software. Moreover, I learned about the rigour needed for good science and improved my science communication skills. Additionally, I experienced an interdisciplinary research laboratory environment, observed how Nuclear Magnetic Resonance (NMR) experiments are designed and carried out, and attended research symposiums and journal clubs which sparked further research ideas that I am excited to pursue. Overall, the experience made me realize that I would enjoy a research-based career and am planning to apply for PhD programmes. I am extremely grateful to the Biochemical Society to have provided me this opportunity.

References.

1. Meisl, G., Yang, X., Hellstrand, E., Frohm, B., Kirkegaard, J. B., Cohen, S. I. *et al.* (2014) Differences in nucleation behavior underlie the contrasting aggregation kinetics of the Abeta40 and Abeta42 peptides Proc Natl Acad Sci U S A **111**, 9384-9389 10.1073/pnas.1401564111
2. Piana, S. (2011) How robust are protein folding simulations with respect to force field parameterization? (vol 100, pg L47, 2011) Biophys J **101**, 1015-1015 10.1016/j.bpj.2011.07.039
3. Heller, G. T., Aprile, F. A., Michaels, T. C. T., Limbocker, R., Perni, M., Ruggeri, F. S. *et al.* (2020) Small-molecule sequestration of amyloid-β as a drug discovery strategy for Alzheimer's disease Sci Adv **6**, ARTN eabb592410.1126/sciadv.abb5924
4. Hopkins, C. W., Le Grand, S., Walker, R. C., andRoitberg, A. E. (2015) Long-Time-Step Molecular Dynamics through Hydrogen Mass Repartitioning J Chem Theory Comput **11**, 1864-1874 10.1021/ct5010406
5. Fossat, M. J., Posey, A. E., andPappu, R. V. (2021) Quantifying charge state heterogeneity for proteins with multiple ionizable residues Biophys J **120**, 5438-5453 10.1016/j.bpj.2021.11.2886
6. Tesei, G., Schulze, T. K., Crehuet, R., andLindorff-Larsen, K. (2021) Accurate model of liquid-liquid phase behavior of intrinsically disordered proteins from optimization of single-chain properties P Natl Acad Sci USA **118**, ARTN e211169611810.1073/pnas.2111696118
7. Tesei, G., andLindorff-Larsen, K. (2022) Improved predictions of phase behaviour of intrinsically disordered proteins by tuning the interaction range Open Res Eur **2**, 94 10.12688/openreseurope.14967.2
8. Tesei, G., Trolle, A. I., Jonsson, N., Betz, J., Knudsen, F. E., Pesce, F. *et al.* (2024) Conformational ensembles of the human intrinsically disordered proteome Nature **626**, 10.1038/s41586-023-07004-5